Available online at www.sciencedirect.com
ScienceDirect
European Journal of Mechanics B/Fluids 26 (2007) 15–27

Series solutions of unsteady three-dimensional MHD flow and heat transfer in the boundary layer over an impulsively stretching plate

Hang Xu [a], Shi-Jun Liao [a,*], Ioan Pop [b]

[a] *School of Naval Architecture, Ocean and Civil Engineering, Shanghai Jiao Tong University, Shanghai 200030, China*
[b] *Faculty of Mathematics, University of Cluj, R-3400 Cluj, CP253, Romania*

Received 9 May 2005; received in revised form 28 October 2005; accepted 20 December 2005

Available online 11 May 2006

Abstract

In this paper, the unsteady boundary-layer flow and heat transfer in an incompressible viscous electrically conducting fluid, caused by an impulsive stretching of the surface in two lateral directions and by suddenly increasing the surface temperature from that of surrounding fluid are studied analytically. By using the homotopy analysis method, the accurate series solutions are obtained which are uniformly valid for all dimensionless time in the whole spatial region $0 \leqslant \eta < \infty$. To the best of our knowledge, such kind of solutions have not been reported.

Keywords: MHD flow; Heat transfer; Unsteady; Boundary-layer; Series solution

1. Introduction

Investigations of boundary layer flow and heat transfer of viscous fluids over a stretching sheet are important in many manufacturing processes, such as polymer extrusion, drawing of copper wires, continuous stretching of plastic films and artificial fibers, hot rolling, wire drawing, glass-fiber, metal extrusion, and metal spinning. Sakiadis [1] firstly studied the boundary layer flow over a stretched surface moving with a constant velocity. Tsou et al. [2] considered the effect of heat transfer on a continuous moving surface with a constant velocity and experimentally confirmed the numerical results of Sakiadis. Erickson et al. [3] extended the work of Sakiadis to include blowing or suction at the stretched sheet surface on a continuous moving surface with a constant speed and investigated its effects on the heat and mass transfer in the boundary layer. Chen and Strobel [4] considered the effect of a buoyancy-induced pressure gradient in a laminar boundary layer of a stretched sheet with constant velocity and temperature. Chakrabarti and Gupta [5] studied the MHD flow of Newtonian fluids initially at rest, over a stretching sheet at a different uniform temperature. Vajravelu and Hadjinicolaou [6] made a analysis to flows and heat transfer characteristics in an electrically conducting fluid near an isothermal sheet. Recently, Liao [7] obtained an accurate series solution of unsteady boundary layer flows over an impulsively stretching plate uniformly valid for all non-dimensional time τ. Cheng and Huang [8] considered the problem of unsteady flows and heat transfer in the laminar boundary on a linearly accelerat-

* Corresponding author.
E-mail addresses: henry629@sjtu.edu.cn (H. Xu), sjliao@sjtu.edu.cn (S.-J. Liao), popi@math.ubbcluj.ro (I. Pop).

0997-7546/$ – see front matter
doi:10.1016/j.euromechflu.2005.12.003

ing surface with suction or blowing in the absence and presence of a heat source or sink. Xu and Liao [9] investigated the unsteady MHD flows of a non-Newtonian fluid over an impulsively stretching flat sheet and presented an accurate series solution.

The homotopy [10] is a basic concept in topology [11]. Based on the homotopy, some numerical techniques such as the continuation method [12] and the homotopy continuation method [13] were developed. In 1992, using the concept of homotopy, Liao [14] proposed an analytic method for highly nonlinear problems, namely the homotopy analysis method (HAM), which was modified step by step [15–19]. Different from perturbation techniques, the homotopy analysis method is independent upon small parameters at all, so that it is valid for highly nonlinear problems, especially those without small/large physical parameters. Besides, it logical contains the non-perturbation techniques such as Lyapunov's artificial small parameter method [20], Adomian decomposition method [21] and δ-expansion method [22], as proved by Liao [23]. The so-called "homotopy perturbation method" [24] proposed in 1999 is only a special case of the homotopy analysis method, as pointed out by Liao [25]. Thus, it is more general and is a unification of previous non-perturbation techniques. Besides, different from all previous analytic methods, the homotopy analysis method always gives us a family of series solutions whose convergence region can be adjusted and controlled by an auxiliary parameter. For details, please refer to Liao [23]. The homotopy analysis method has been successfully applied to many types of nonlinear problems [7,9,23,26–30]. Some new solutions of a few nonlinear problems [31,32] are even found by means of it. The aim of the present paper is to study analytically the unsteady three-dimensional MHD flow and heat transfer in the boundary layer over an impulsively stretching flat plate. To the best of our knowledge, no one has reported such accurate series solutions which are valid for all dimensionless time $0 \leqslant \tau < \infty$ in the whole spatial region $0 \leqslant \eta < \infty$.

2. Mathematical description

Consider the unsteady, three-dimensional laminar flow of an electrically conducting fluid caused by an impulsive stretching flat surface in two lateral directions in an otherwise quiescent fluid in the presence of a transverse magnetic field. It is assumed that at time $t = 0$, the flat plate and the fluid are at rest and they have the same constant temperature T_∞. Then at time $t = 0$, the flat plate is stretched with the velocity $u_w = ax$ and $v_w = by$. At the same time the surface temperature is raised from T_∞ to the constant value T_w, where $T_w > T_\infty$. It is assumed that the magnetic Reynolds number is small. Under these conditions the governing equations for the unsteady boundary layer flow and heat transfer for this problem are (see [33])

$$\frac{\partial u}{\partial x} + \frac{\partial v}{\partial y} + \frac{\partial w}{\partial z} = 0, \tag{1}$$

$$\frac{\partial u}{\partial t} + u\frac{\partial u}{\partial x} + v\frac{\partial u}{\partial y} + w\frac{\partial u}{\partial z} = \nu\frac{\partial^2 u}{\partial z^2} - \frac{\sigma B^2}{\rho}u, \tag{2}$$

$$\frac{\partial v}{\partial t} + u\frac{\partial v}{\partial x} + v\frac{\partial v}{\partial y} + w\frac{\partial v}{\partial z} = \nu\frac{\partial^2 v}{\partial z^2} - \frac{\sigma B^2}{\rho}v, \tag{3}$$

$$\frac{\partial T}{\partial t} + u\frac{\partial T}{\partial x} + v\frac{\partial T}{\partial y} + w\frac{\partial T}{\partial z} = \alpha\frac{\partial^2 T}{\partial z^2}, \tag{4}$$

where u, v and w are the velocity components in the x-, y- and z-directions, t denotes the time, ρ, σ, B and α are the density, electrical conductivity, magnetic field and the thermal diffusivity of the fluid, respectively. The corresponding initial and boundary conditions are

$$t < 0: \quad u = v = w = Q, \quad T = T_\infty, \tag{5a}$$

$$t \geqslant 0: \quad u = ax, \quad v = by, \quad w = 0, \quad T = T_w \quad \text{at } z = 0, \tag{5b}$$

$$t \geqslant 0: \quad u \to 0, \quad v \to 0, \quad T \to 0 \quad \text{as } z \to +\infty, \tag{5c}$$

here, a and b are positive constants. Following Williams and Rhyne [34] and Takhar [33], we use the similarity transformations

$$\eta = z\sqrt{\frac{a}{\nu\xi}}, \quad \xi = 1 - \exp(-\tau), \quad \tau = at,$$
$$u = ax\frac{\partial f}{\partial \eta}, \quad v = by\frac{\partial s}{\partial \eta}, \quad w = -\sqrt{a\nu\xi}\,(f + s), \quad g = \frac{T - T_\infty}{T_w - T_\infty}. \tag{6}$$

Then, the governing equations (1)–(4) become

$$(1-\xi)\left(\frac{\eta}{2}f'' - \xi\frac{\partial f'}{\partial \xi}\right) + f''' + \xi\left[(f+s)f'' - (f')^2 - Mf'\right] = 0, \tag{7}$$
$$(1-\xi)\left(\frac{\eta}{2}s'' - \xi\frac{\partial s'}{\partial \xi}\right) + s''' + \xi\left[(f+s)s'' - (s')^2 - Ms'\right] = 0, \tag{8}$$
$$(1-\xi)\left(\frac{\eta}{2}g' - \xi\frac{\partial g}{\partial \xi}\right) + \frac{1}{Pr}g'' + \xi(f+s)g' = 0, \tag{9}$$

subject to the boundary conditions

$$f(0,\xi) = s(0,\xi) = 0, \quad g(0,\xi) = f'(0,\xi) = 1, \quad s'(0,\xi) = c, \quad g(\infty,\xi) = f'(\infty,\xi) = s'(\infty,\xi) = 0, \tag{10}$$

where primes denote differentiation with respect to η, $c = b/a$ is a positive constant, $M = \sigma B^2/(\rho a)$ is the magnetic parameter and $Pr = \nu/a$ is the Prandtl number.

When $\xi = 0$, corresponding to $\tau = 0$, we have from (7), (8) and (9) that

$$f''' + \frac{\eta}{2}f'' = 0, \tag{11}$$
$$s''' + \frac{\eta}{2}s'' = 0, \tag{12}$$
$$\frac{1}{Pr}g'' + \frac{\eta}{2}g' = 0, \tag{13}$$

subject to the boundary conditions (10) for $\xi = 0$. The above equations (11), (12) and (13) have the exact solutions

$$f(\eta,0) = \eta\,\mathrm{erfc}\left(\frac{\eta}{2}\right) + \frac{2}{\sqrt{\pi}}\left[1 - \exp\left(-\frac{\eta^2}{4}\right)\right], \tag{14}$$
$$s(\eta,0) = c\left\{\eta\,\mathrm{erfc}\left(\frac{\eta}{2}\right) + \frac{2}{\sqrt{\pi}}\left[1 - \exp\left(-\frac{\eta^2}{4}\right)\right]\right\}, \tag{15}$$
$$g(\eta,0) = \mathrm{erfc}\left(\frac{\sqrt{Pr}\,\eta}{2}\right), \tag{16}$$

where

$$\mathrm{erfc}(\eta) = 1 - \frac{2}{\sqrt{\pi}}\int_0^\eta \exp\left(-x^2\right)\mathrm{d}x. \tag{17}$$

When $\xi = 1$, corresponding to $\tau \to +\infty$, Eqs. (7), (8) and (9) reduce to

$$f''' + (f+s)f'' - (f')^2 - Mf' = 0, \tag{18}$$
$$s''' + (f+s)s'' - (s')^2 - Ms' = 0, \tag{19}$$
$$\frac{1}{Pr}g'' + (f+s)g' = 0, \tag{20}$$

subject to the boundary conditions (10) for $\xi = 1$.

3. Homotopy analysis solution

3.1. Zeroth-order deformation equation

In general, asymptotic solutions of boundary-layer flows over a stretching plate decay exponentially at infinity (refer to [23] and [33]). Further, Liao [7] obtained accurate solutions of a kind of unsteady boundary layer flows in a Newtonian fluid caused by an impulsively stretching flat plate. Following Takhar [33] and Liao [7], we express $f(\eta,\xi)$, $s(\eta,\xi)$ and $g(\eta,\xi)$ by a set of base functions

$$\left\{\xi^k\eta^j\exp(-n\gamma\eta)\mid k\geqslant 0,\ n\geqslant 0,\ j\geqslant 0\right\} \tag{21}$$

in the form

$$f(\eta,\xi)=a_{0,0}^0+\sum_{k=0}^{+\infty}\sum_{j=0}^{+\infty}\sum_{n=1}^{+\infty}a_{j,n}^k\xi^k\eta^j\exp(-n\gamma\eta), \tag{22a}$$

$$s(\eta,\xi)=b_{0,0}^0+\sum_{k=0}^{+\infty}\sum_{j=0}^{+\infty}\sum_{n=1}^{+\infty}b_{j,n}^k\xi^k\eta^j\exp(-n\gamma\eta), \tag{22b}$$

$$g(\eta,\xi)=\sum_{k=0}^{+\infty}\sum_{j=0}^{+\infty}\sum_{n=1}^{+\infty}c_{j,n}^k\xi^k\eta^j\exp(-n\gamma\eta), \tag{22c}$$

where $a_{j,n}^k$, $b_{j,n}^k$ and $c_{j,n}^k$ are coefficients, γ is a spatial-scale parameter. These provide us with the *Solution Expressions* for $f(\eta,\xi)$, $s(\eta,\xi)$ and $g(\eta,\xi)$. On basis of the *Solution Expressions* (22a)–(22c) and from the boundary conditions (10), it is straightforward to choose

$$f_0(\eta,\xi)=\frac{1-\exp(-\gamma\eta)}{\gamma}, \tag{23a}$$

$$s_0(\eta,\xi)=\frac{c[1-\exp(-\gamma\eta)]}{\gamma}, \tag{23b}$$

$$g_0(\eta,\xi)=\exp(-\gamma\eta), \tag{23c}$$

as the initial approximations of $f(\eta,\xi)$, $s(\eta,\xi)$ and $g(\eta,\xi)$ besides to choose

$$\mathcal{L}_f\left[\Phi(\xi,\eta;q)\right]=\frac{\partial^3\Phi}{\partial\eta^3}-\gamma^2\frac{\partial\Phi}{\partial\eta}, \tag{24a}$$

$$\mathcal{L}_s\left[\Theta(\xi,\eta;q)\right]=\frac{\partial^3\Theta}{\partial\eta^3}-\gamma^2\frac{\partial\Theta}{\partial\eta}, \tag{24b}$$

$$\mathcal{L}_g\left[\Psi(\xi,\eta;q)\right]=\frac{\partial^2\Psi}{\partial\eta^2}-\gamma^2\Psi, \tag{24c}$$

as the auxiliary linear operators, which have the following properties

$$\mathcal{L}_f\left[C_1\exp(-\gamma\eta)+C_2\exp(\gamma\eta)+C_3\right]=0, \tag{25a}$$

$$\mathcal{L}_s\left[C_4\exp(-\gamma\eta)+C_5\exp(\gamma\eta)+C_6\right]=0, \tag{25b}$$

$$\mathcal{L}_g\left[C_7\exp(-\gamma\eta)+C_8\exp(\gamma\eta)\right]=0, \tag{25c}$$

where C_1, C_2, C_3, C_4, C_5, C_6, C_7 and C_8 are constants. According to the base function denoted by (21), we can first decide the solution expressions of $f(\eta,\xi)$, $s(\eta,\xi)$ and $g(\eta,\xi)$. Then we can choose initial guesses $f_0(\eta,\xi)$, $s_0(\eta,\xi)$ and $g_0(\eta,\xi)$ based on the solution expressions defined by (22a)–(22c) and the boundary conditions (10). Note also that we have freedom to choose the different initial guesses of $f_0(\eta)$, $s_0(\eta)$ and $g_0(\eta)$ as long as they satisfy the *Solution Expressions* denoted by (22a)–(22c) and the boundary conditions (10). For the convenience of symbol calculation (it is a prominent merit of the HAM), we usually choose them as simple as possible. The linear operators can be chosen on basis of two rules. Firstly, they must satisfy the solution expressions denoted by (22a)–(22c). The basic solutions of these linear operators should be only contained (at most) the four terms η, $\exp(-\eta)$, $\exp(\eta)$ or constant. Secondly, to decide the basic solutions of these linear operators, all of boundary conditions in (10) must be used to determine integral constants. Note that we also have freedom to choose the linear operators as long as they satisfy above-mentioned rules. For details, the readers are referred to [23].

Based on (7), (8) and (9), we are led to define the nonlinear operators

$$\mathcal{N}_f\big[\Phi(\eta,\xi;q)\big]=(1-\xi)\left(\frac{\eta}{2}\frac{\partial^2\Phi}{\partial\eta^2}-\xi\frac{\partial^2\Phi}{\partial\eta\partial\xi}\right)+\frac{\partial^3\Phi}{\partial\eta^3}+\xi\left[(\Phi+\Theta)\frac{\partial^2\Phi}{\partial\eta^2}-\left(\frac{\partial\Phi}{\partial\eta}\right)^2-M\frac{\partial\Phi}{\partial\eta}\right], \tag{26a}$$

$$\mathcal{N}_s\big[\Theta(\eta,\xi;q)\big]=(1-\xi)\left(\frac{\eta}{2}\frac{\partial^2\Theta}{\partial\eta^2}-\xi\frac{\partial^2\Theta}{\partial\eta\partial\xi}\right)+\frac{\partial^3\Theta}{\partial\eta^3}+\xi\left[(\Phi+\Theta)\frac{\partial^2\Theta}{\partial\eta^2}-\left(\frac{\partial\Theta}{\partial\eta}\right)^2-M\frac{\partial\Theta}{\partial\eta}\right], \tag{26b}$$

$$\mathcal{N}_g\big[\Psi(\eta,\xi;q)\big]=(1-\xi)\left(\frac{\eta}{2}\frac{\partial\Psi}{\partial\eta}-\xi\frac{\partial\Psi}{\partial\xi}\right)+\frac{1}{Pr}\frac{\partial^2\Psi}{\partial\eta^2}+\xi(\Phi+\Theta)\frac{\partial\Psi}{\partial\eta}. \tag{26c}$$

Let $\hbar_f$, $\hbar_s$ and $\hbar_g$ denote the non-zero auxiliary parameters. We construct the zeroth-order deformation equations

$$(1-q)\mathcal{L}_f\big[\Phi(\eta,\xi;q)-f_0(\eta,\xi)\big]=q\hbar_f\mathcal{N}_f\big[\Phi(\eta,\xi;q)\big], \tag{27a}$$

$$(1-q)\mathcal{L}_s\big[\Theta(\eta,\xi;q)-s_0(\eta,\xi)\big]=q\hbar_s\mathcal{N}_s\big[\Theta(\eta,\xi;q)\big], \tag{27b}$$

$$(1-q)\mathcal{L}_g\big[\Psi(\eta,\xi;q)-g_0(\eta,\xi)\big]=q\hbar_g\mathcal{N}_g\big[\Psi(\eta,\xi;q)\big], \tag{27c}$$

subject to the boundary conditions

$$\begin{aligned}&\Phi(0,\xi)=\Theta(0,\xi),\quad \Psi(0,\xi)=\left.\frac{\partial\Phi(\eta,\xi)}{\partial\eta}\right|_{\eta=0}=1,\quad \left.\frac{\partial\Theta(\eta,\xi)}{\partial\eta}\right|_{\eta=0}=c,\\&\Psi(\infty,\xi)=\left.\frac{\partial\Phi(\eta,\xi)}{\partial\eta}\right|_{\eta\to+\infty}=\left.\frac{\partial\Theta(\eta,\xi)}{\partial\eta}\right|_{\eta\to+\infty}=0,\end{aligned} \tag{28}$$

where $q\in[0,1]$ is an embedding parameter.

Obviously, when $q=0$ and $q=1$, the above zeroth-order deformation equations (27a)–(27c) have the solutions

$$\Phi(\eta,\xi;0)=f_0(\eta,\xi),\quad \Theta(\eta,\xi;0)=s_0(\eta,\xi),\quad \Psi(\eta,\xi;0)=g_0(\eta,\xi), \tag{29a}$$

and

$$\Phi(\eta,\xi;1)=f(\eta,\xi),\quad \Theta(\eta,\xi;1)=s(\eta,\xi),\quad \Psi(\eta,\xi;1)=g(\eta,\xi), \tag{29b}$$

respectively. Thus as q increases from 0 to 1, $\Phi(\eta,\xi;q)$, $\Theta(\eta,\xi;q)$ and $\Psi(\eta,\xi;q)$ vary from the initial guesses $f_0(\eta,\xi)$, $s_0(\eta,\xi)$ and $g_0(\eta,\xi)$ to the solutions $f(\eta,\xi)$, $s(\eta,\xi)$ and $g(\eta,\xi)$ of the considered unsteady problem, respectively. So, expanding $\Phi(\eta,\xi;q)$, $\Theta(\eta,\xi;q)$ and $\Psi(\eta,\xi;q)$ in Taylor's series with respect to the embedding parameter q, we have

$$\Phi(\eta,\xi;q)=\Phi(\eta,\xi,0)+\sum_{m=1}^{+\infty}f_m(\eta,\xi)q^m, \tag{30a}$$

$$\Theta(\eta,\xi;q)=\Theta(\eta,\xi,0)+\sum_{m=1}^{+\infty}s_m(\eta,\xi)q^m, \tag{30b}$$

$$\Psi(\eta,\xi;q)=\Psi(\eta,\xi,0)+\sum_{m=1}^{+\infty}g_m(\eta,\xi)q^m, \tag{30c}$$

where

$$f_m(\eta,\xi)=\frac{1}{m!}\left.\frac{\partial^m\Phi(\eta,\xi;q)}{\partial q^m}\right|_{q=0}, \tag{31a}$$

$$s_m(\eta,\xi)=\frac{1}{m!}\frac{\partial^m\Theta(\eta,\xi;q)}{\partial q^m}\bigg|_{q=0}, \tag{31b}$$

$$g_m(\eta,\xi)=\frac{1}{m!}\frac{\partial^m\Psi(\eta,\xi;q)}{\partial q^m}\bigg|_{q=0}. \tag{31c}$$

Note that (27a), (27b) and (27c) contain the auxiliary parameter $\hbar_f$, $\hbar_s$ and $\hbar_g$. Assuming that $\hbar_f$, $\hbar_s$ and $\hbar_g$ are properly chosen so that the series (30a)–(30c) are convergent at $q=1$, we have, using (29a) and (29b), the solution series

$$f(\eta,\xi)=f_0(\eta,\xi)+\sum_{m=1}^{+\infty}f_m(\eta,\xi), \tag{32a}$$

$$s(\eta,\xi)=s_0(\eta,\xi)+\sum_{m=1}^{+\infty}s_m(\eta,\xi), \tag{32b}$$

$$g(\eta,\xi)=g_0(\eta,\xi)+\sum_{m=1}^{+\infty}g_m(\eta,\xi). \tag{32c}$$

3.2. High-order deformation equation

For simplicity, we define the vector

$$\vec{f}_m=\{f_0,f_1,\ldots,f_m\},\quad \vec{s}_m=\{s_0,s_1,\ldots,s_m\},\quad \vec{g}_m=\{g_0,g_1,\ldots,g_m\}. \tag{33}$$

Differentiating the zeroth-order deformation equations (27a)–(27c) m times with respect to q, then setting $q=0$, and finally dividing them by $m!$, we obtain the mth-order deformation equations

$$\mathcal{L}\big[f_m(\eta,\xi)-\chi_m f_{m-1}(\eta,\xi)\big]=\hbar_f R_m(\vec{f}_{m-1}), \tag{34a}$$

$$\mathcal{L}_s\big[s_m(\eta,\xi)-\chi_m s_{m-1}(\eta,\xi)\big]=\hbar_s S_m(\vec{s}_{m-1}), \tag{34b}$$

$$\mathcal{L}_g\big[g_m(\eta,\xi)-\chi_m g_{m-1}(\eta,\xi)\big]=\hbar_g W_m(\vec{g}_{m-1}), \tag{34c}$$

subject to the boundary conditions

$$f_m(0,\xi)=s_m(0,\xi)=g_m(0,\xi)=f'_m(0,\xi)=s'_m(0,\xi)=0,\qquad g_m(\infty,\xi)=f'_m(\infty,\xi)=s'_m(\infty,\xi)=0, \tag{35}$$

where

$$\begin{aligned}R_m(\vec{f}_{m-1})&=\frac{1}{(m-1)!}\frac{\partial^{m-1}\mathcal{N}_f[\Phi(\eta,\xi;q)]}{\partial q^{m-1}}\bigg|_{q=0}\\&=(1-\xi)\left(\frac{\eta}{2}f''_{m-1}-\xi\frac{\partial f'_{m-1}}{\partial\xi}\right)+f'''_{m-1}\\&\quad+\xi\left[\sum_{i=0}^{k-1}\big(f_i f''_{m-1-i}+s_i f''_{m-1-i}-f_i f'_{m-1-i}\big)-Mf'_{m-1}\right],\end{aligned} \tag{36a}$$

$$\begin{aligned}S_m(\vec{s}_{m-1})&=\frac{1}{(m-1)!}\frac{\partial^{m-1}\mathcal{N}_s[\Theta(\eta,\xi;q)]}{\partial q^{m-1}}\bigg|_{q=0}\\&=(1-\xi)\left(\frac{\eta}{2}s''_{m-1}-\xi\frac{\partial s'_{m-1}}{\partial\xi}\right)+s'''_{m-1}\\&\quad+\xi\left[\sum_{i=0}^{k-1}\big(s_i s''_{m-1-i}+f_i s''_{m-1-i}-s_i s'_{m-1-i}\big)-Ms'_{m-1}\right],\end{aligned} \tag{36b}$$

$$W_m(\vec{g}_{m-1}) = \frac{1}{(m-1)!}\frac{\partial^{m-1}\mathcal{N}_g[\Psi(\eta,\xi;q)]}{\partial q^{m-1}}\bigg|_{q=0}$$
$$= (1-\xi)\left(\frac{\eta}{2}g'_{m-1} - \xi\frac{\partial g_{m-1}}{\partial \xi}\right) + \frac{1}{Pr}g''_{m-1} + \xi\sum_{i=0}^{m-1}\left(f_i g'_{m-1-i} + s_i g'_{m-1-i}\right), \tag{36c}$$

and

$$\chi_m = \begin{cases} 0, & m=1, \\ 1, & m>1. \end{cases} \tag{37}$$

Let $f_m^*(\eta,\xi)$, $s_m^*(\eta,\xi)$ and $g_m^*(\eta,\xi)$ denote the particular solutions of (34a)–(34c). Using (25a)–(25c), we have the general solutions

$$f_m(\eta,\xi) = f_m^*(\eta,\xi) + C_1\exp(-\gamma\eta) + C_2\exp(\gamma\eta) + C_3, \tag{38a}$$

$$s_m(\eta,\xi) = s_m^*(\eta,\xi) + C_4\exp(-\gamma\eta) + C_5\exp(\gamma\eta) + C_6, \tag{38b}$$

$$g_m(\eta,\xi) = g_m^*(\gamma\eta,\xi) + C_7\exp(-\gamma\eta) + C_8\exp(\gamma\eta), \tag{38c}$$

where the coefficients C_1, C_2, C_3, C_4, C_5, C_6, C_7 and C_8 are determined by the boundary conditions (35), i.e.

$$C_2 = C_5 = C_8 = 0, \quad C_1 = \frac{1}{\gamma}\frac{\partial f_m^*(\eta,\xi)}{\partial\eta}\bigg|_{\eta=0}, \quad C_3 = -C_1 - f_m^*(0,\xi),$$
$$C_4 = \frac{1}{\gamma}\frac{\partial s_m^*(\eta,\xi)}{\partial\eta}\bigg|_{\eta=0}, \quad C_6 = -C_4 - s_m^*(0,\xi), \quad C_7 = -g_m^*(0,\xi). \tag{39}$$

In this way, it is easy to solve the *linear* equations (34a)–(34c) after the other in the order $m = 1, 2, 3, \ldots$ by means of the symbolic computation software such as Mathematica, Maple.

4. Analysis of results

It should be emphasized that the solution series (32a)–(32c) contain four auxiliary parameters $\hbar_f$, $\hbar_s$, $\hbar_g$ and γ, which can be determined in the way described below. To decide the auxiliary parameter γ, we define a kind of error function as

$$E(\gamma) = \int_0^1\int_0^{+\infty}\left[R_1(\vec{f_0})\right]^2\,\mathrm{d}\eta\,\mathrm{d}\xi, \tag{40}$$

where $R_1(\vec{f_0})$ is determined by Eq. (36a). Let

$$\frac{\mathrm{d}E(\gamma)}{\mathrm{d}\gamma} = 0. \tag{41}$$

Then, we can obtain a proper value of parameter γ by solving Eq. (41). To decide the auxiliary parameters $\hbar_f$, $\hbar_s$ and $\hbar_g$, we assume $\hbar_s = \hbar_g = \hbar_f$. Thus, the analytic approximations of $f(\eta,\xi)$, $s(\eta,\xi)$ and $g(\eta,\xi)$ now are the functions of η, ξ and $\hbar_f$. So are the derivatives of $f(\eta,\xi)$, $s(\eta,\xi)$ and $g(\eta,\xi)$. Given any prescribed values of $\eta = \eta^*$ and $\xi = \xi^*$, the analytic approximations of $f(\eta^*,\xi^*)$, $s(\eta^*,\xi^*)$ and $g(\eta^*,\xi^*)$ and their derivatives now are only dependent on $\hbar_f$. Then, by plotting the curves of $f''(\eta^*,\xi^*)$ versus $\hbar_f$ (which is called the $\hbar$-curve for $f''(\eta^*,\xi^*)$), we can obtain a valid region $\hbar_f^{\min} \leqslant \hbar_f \leqslant \hbar_f^{\max}$. The $\hbar_f$ can then be chosen in the region $[\hbar_f^{\min}, \hbar_f^{\max}]$. Repeating the above-mentioned processes, the proper values of $\hbar_s$ and $\hbar_g$ can be decided, accordingly. For more details, the readers are referred to [23]. Note that all auxiliary parameters in our calculation should be integer so that the calculation errors due to the precision of digital computer can be reduced. The values of parameters $\hbar_f$, $\hbar_s$, $\hbar_g$ and γ used in our analysis are listed in Table 1.

When $\xi = 0$, corresponding to the initial state, our analytic approximations agree well with the exact solutions (14)–(16), as shown in Figs. 1–3. When $\xi = 1$, corresponding to the steady-state, our analytic approximations agree well with the numerical ones, as shown in Figs. 4–6. In a similar way, it is found that the solution series (32a)–(32c)

Table 1
The values of parameters used in our calculation

$M = 0, 1, 3, 5,\ c = 0, 1/4, 1/2, 3/4, 1$			
	$Pr = 0.72$	$Pr = 3$	$Pr = 7$
$\hbar_f$	$-1/4$	$-3/2$	$-3/2$
$\hbar_s$	$-1/4$	$-3/2$	$-3/2$
$\hbar_g$	$-1/4$	-2	-2
γ	1	3	3

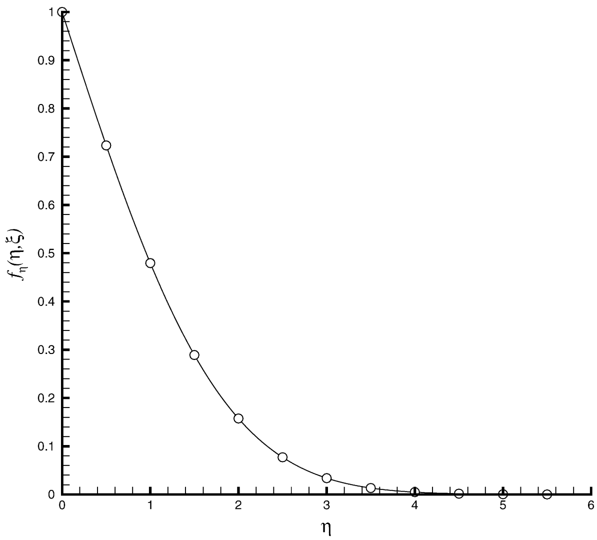

Fig. 1. The comparison of $f_\eta(\eta, \xi)$ of the analytic approximation with the exact solution at $\xi = 0$. Open circles: exact solution; Solid line: 25th-order HAM approximation.

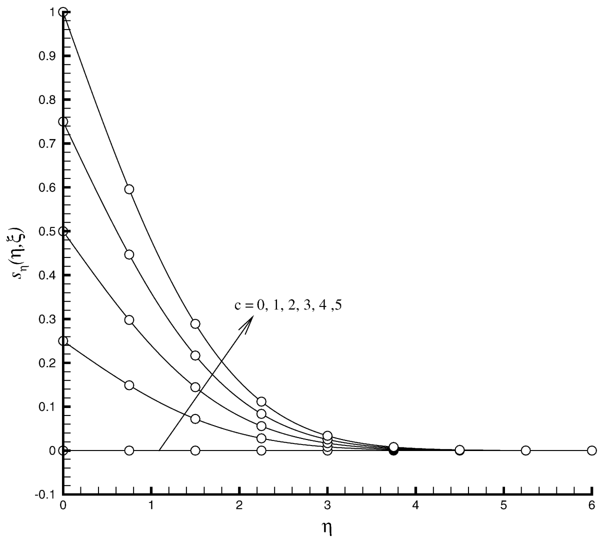

Fig. 2. The comparisons of $s_\eta(\eta, \xi)$ of the analytic approximations with the exact solutions at $\xi = 0$ for the different parameter c. Open circles: exact solutions; Solid line: 25th-order HAM approximations.

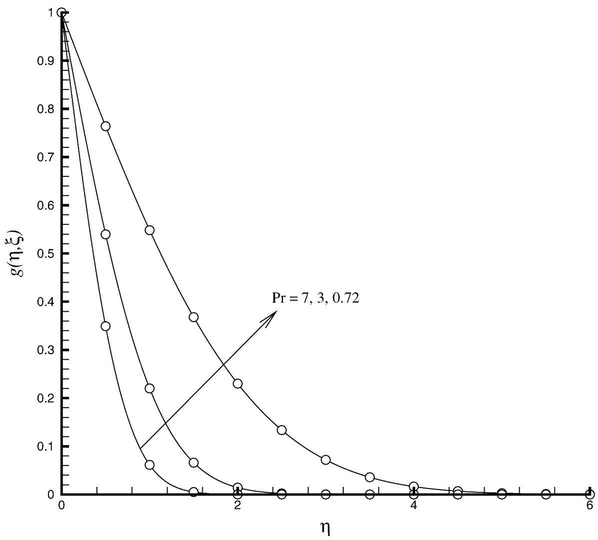

Fig. 3. The comparisons of $g(\eta, \xi)$ of the analytic approximations with the exact solutions at $\xi = 0$ for the different parameter Pr. Open circles: exact solutions; Solid line: 25th-order HAM approximations.

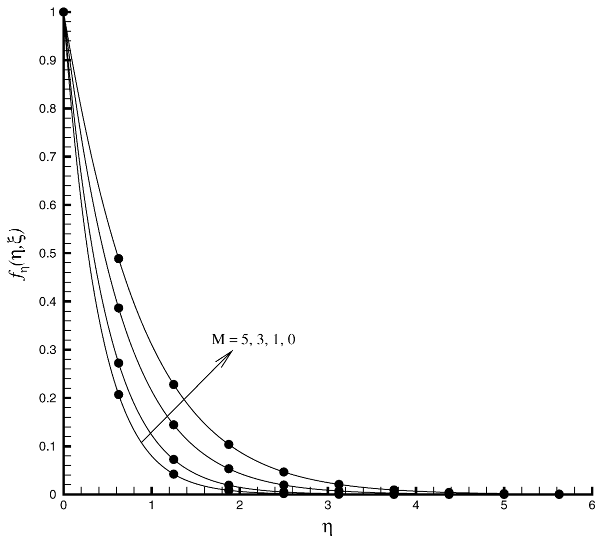

Fig. 4. The comparison of $f_n(\eta, \xi)$ of the analytic approximations with the numerical solutions at $\xi = 1$ for the different parameter M when $c = 0.5$. Filled circle: numerical solutions; Solid line: 25th-order HAM approximations.

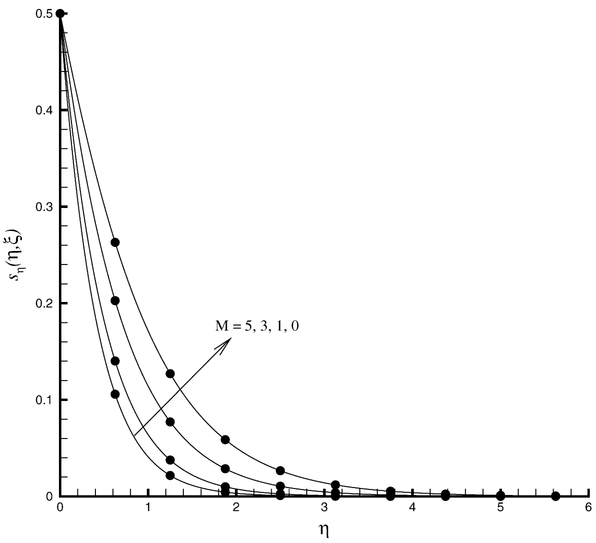

Fig. 5. The comparison of $s_\eta(\eta,\xi)$ of the analytic approximations with the numerical solutions at $\xi=1$ for the different parameter M when $c=0.5$. Filled circle: numerical solutions; Solid line: 25th-order HAM approximations.

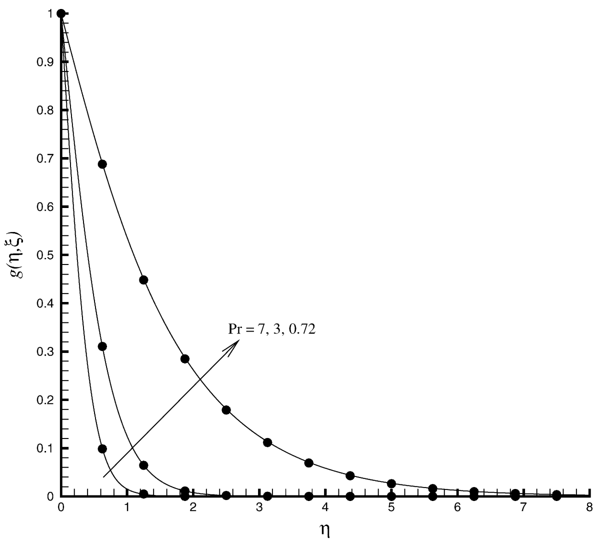

Fig. 6. The comparison of $g(\eta,\xi)$ of the analytic approximations with the numerical solutions at $\xi=1$ for the different parameter Pr when $c=0.5$ and $M=1$. Filled circle: numerical solutions; Solid line: 25th-order HAM approximations.

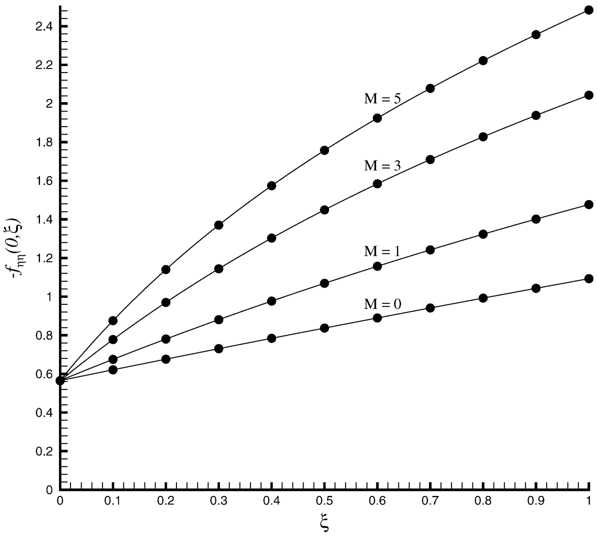

Fig. 7. The analytic approximations of $-f_{\eta\eta}(0,\xi)$ for $0\leqslant\xi\leqslant1$ for different M when $c=0.5$. Solid line: 20th-order HAM approximations; Filled circles: 25th-order HAM approximations.

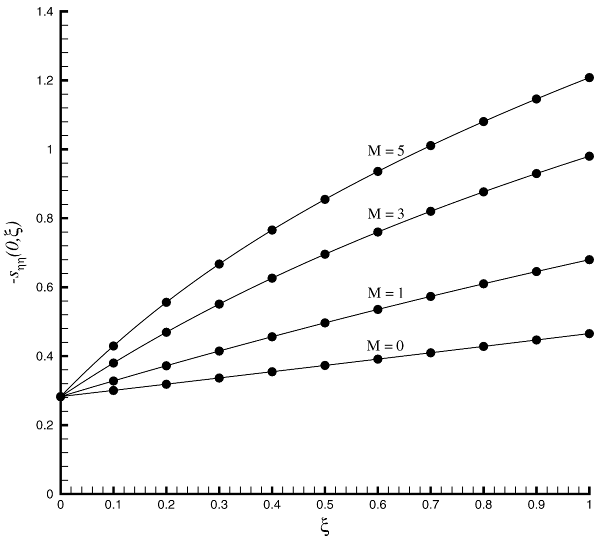

Fig. 8. The analytic approximations of $-s_{\eta\eta}(0,\xi)$ for $0\leqslant\xi\leqslant1$ for different M when $c=0.5$. Solid line: 20th-order HAM approximations; Filled circles: 25th-order HAM approximations.

are convergent in the whole range of the dimensionless time $\xi\in[0,1]$ for all considered cases of M, c and Pr, as shown in Figs. 7–13. Thus, by means of homotopy analysis method, we obtain series solutions which are accurate and uniformly valid for all dimensionless time $\xi\in[0,1]$ in the whole spatial region $0\leqslant\eta<+\infty$. Such kind of series solutions have not been reported, to the best of our knowledge.

It is found from Figs. 7–9 that, at the start of the motion ($\xi=0$), the surface shear stresses in the x- and y-directions ($-f_{\eta\eta}(0,\xi)$, $-s_{\eta\eta}(0,\xi)$) and the surface heat transfer ($-g_\eta(0,\xi)$) are independent on M, because M is multiplied by ξ (see Eqs. (7)–(9)). Therefore, M increases as ξ increases. The surface shear stresses increase as the magnetic parameter M increases, because the enhanced Lorentz force which imparts additional momentum into the boundary layer. This reduces the boundary-layer thickness which, in turn, increases the thermal boundary-layer thickness.

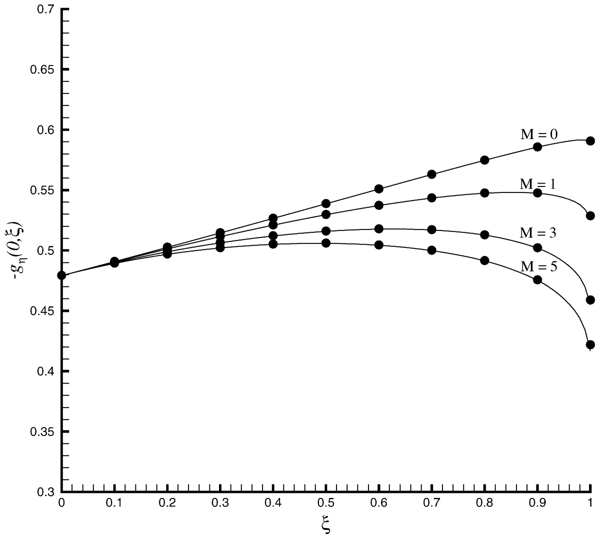

Fig. 9. The analytic approximations of $-g_\eta(0,\xi)$ for $0 \leqslant \xi < 1$ for different M when $c = 0.5$ and $Pr = 0.72$. Solid line: 20th-order HAM approximations; Filled circles: 25th-order HAM approximations.

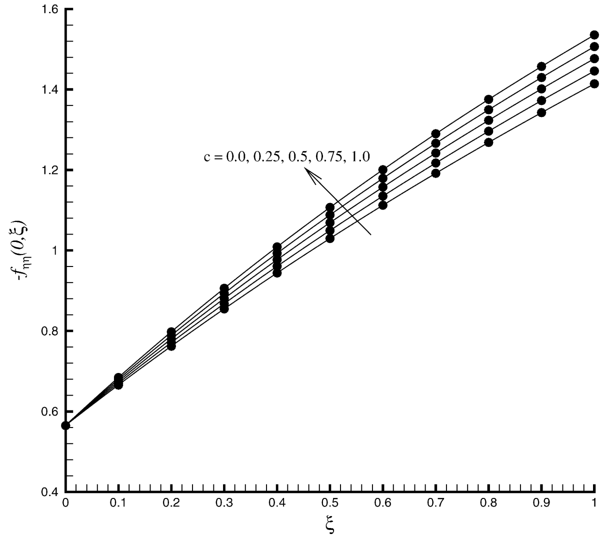

Fig. 10. The analytic approximations of $-f_{\eta\eta}(0,\xi)$ for $0 \leqslant \xi \leqslant 1$ for different c when $M = 1$. Solid line: 20th-order HAM approximations; Filled circles: 25th-order HAM approximations.

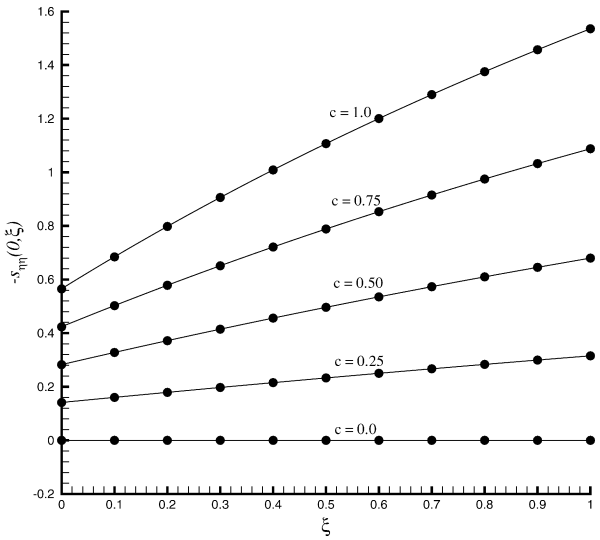

Fig. 11. The analytic approximations of $-s_{\eta\eta}(0,\xi)$ for $0 \leqslant \xi \leqslant 1$ for different c when $M = 1$. Solid line: 20th-order HAM approximations; Filled circles: 25th-order HAM approximations.

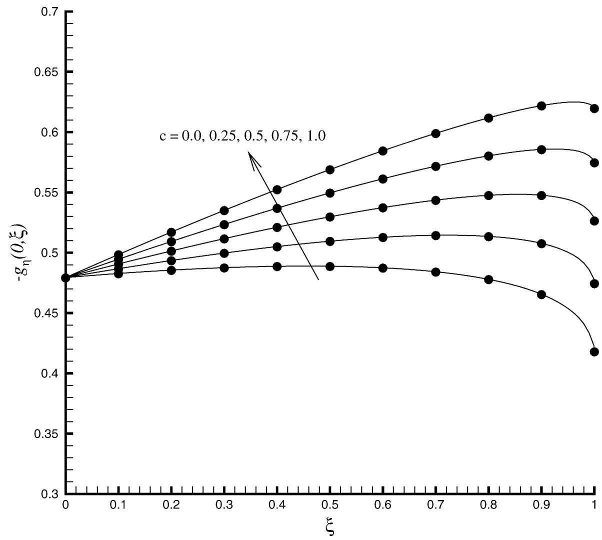

Fig. 12. The analytic approximations of $-g_\eta(0,\xi)$ for $0 \leqslant \xi \leqslant 1$ for different c when $M = 1$ and $Pr = 0.72$. Solid line: 20th-order HAM approximations; Filled circles: 25th-order HAM approximations.

The variation of the surface shear stresses in x- and y-directions and the surface heat transfer $(-f_{\eta\eta}(0,\xi), -s_{\eta\eta}(0,\xi), -g_\eta(0,\xi))$ with dimensionless time ξ, for several values of the stretching parameter c $(0 \leqslant c \leqslant 1)$ when $M = 1$, $Pr = 0.72$, is drawn in Figs. 10–12. Especially, when $c = 0$, the problem reduces to the two-dimensional case. The surface shear stresses in x- and y-directions $(-f_{\eta\eta}(0,\xi), -s_{\eta\eta}(0,\xi))$ increase with ξ almost linearly when $0 \leqslant c \leqslant 1$. The surface heat transfer $(-g_\eta(0,\xi))$ increases with ξ for $\xi \leqslant \xi_0$ $(\xi_0 \approx 0.8)$. Beyond this value, it decreases. The surface shear stresses and the surface heat transfer also increase as the stretching parameter c increases, because increasing c implies higher surface velocity which accelerates the fluid in the boundary-layer. The variation of the surface heat transfer $(-g_\eta(0,\xi))$ with dimensionless time ξ, for several values of the Prandlt number Pr when $M = 1$, $c = 0.5$, is drawn in Fig. 13. It is found that as the Prandtl number increases, the surface heat transfer increases, too.

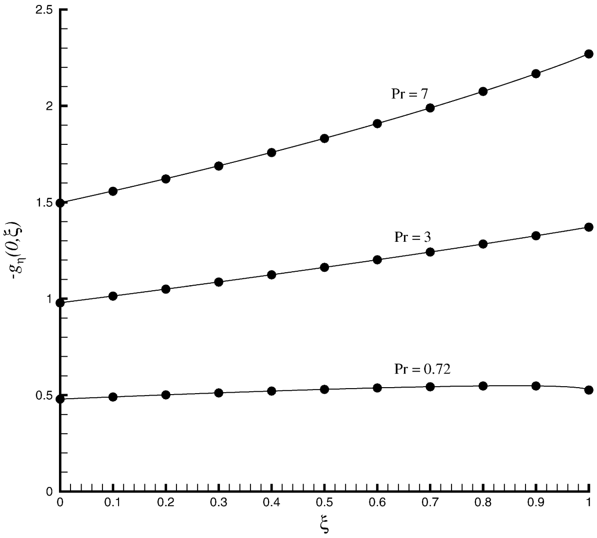

Fig. 13. The analytic approximations of $-g_\eta(0,\xi)$ for $0 \leqslant \xi \leqslant 1$ for different Pr when $M = 1$ and $c = 0.5$. Solid line: 20th-order HAM approximations; Filled circles: 25th-order HAM approximations.

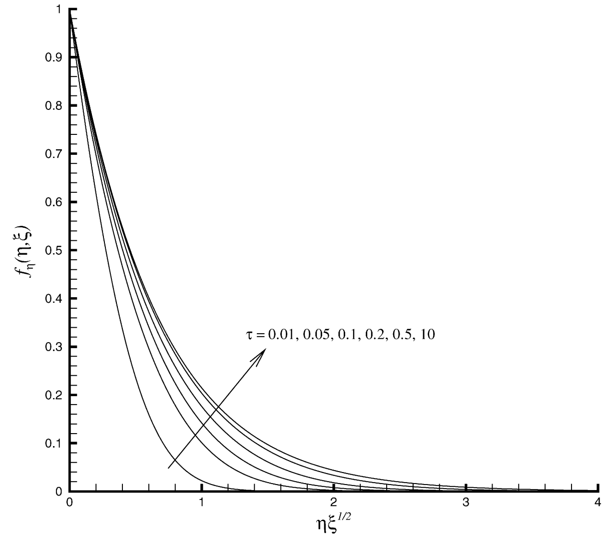

Fig. 14. The variation of the velocity profile $f_\eta(\eta,\xi)$ when $M = 1$ and $c = 0.5$.

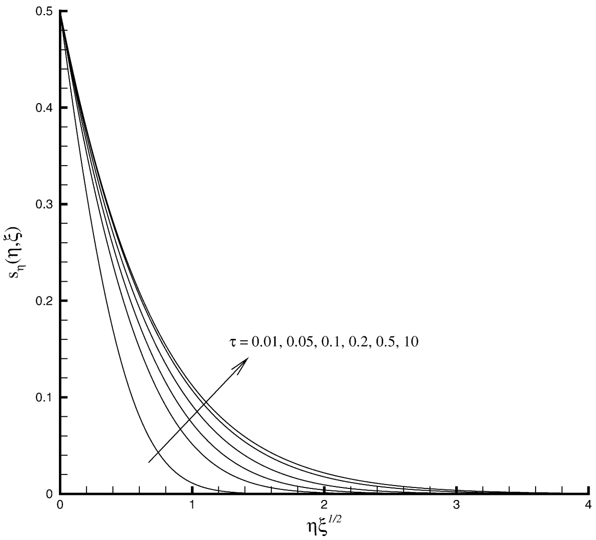

Fig. 15. The variation of the velocity profile $s_\eta(\eta,\xi)$ when $M = 1$ and $c = 0.5$.

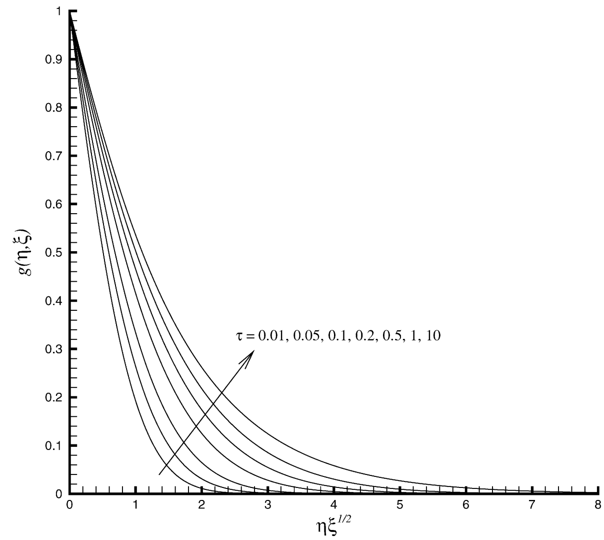

Fig. 16. The variation of the temperature profile $g(\eta,\xi)$ when $M = 1$, $c = 0.5$ and $Pr = 0.72$.

The development of the velocity profiles in the x- and y-directions $(f_\eta(\eta,\xi), s_\eta(\eta,\xi))$ and the temperature profiles $(g(\eta,\xi))$ for $c = 0.5$, $M = 1$ and $Pr = 0.72$ is shown in Figs. 14–16. We can see that these profiles become smoothly as τ increases from zero to ∞.

5. Conclusions

In this paper, the homotopy analysis method is employed to study the unsteady three-dimensional magnetohydrodynamic boundary layer flows with heat transfer over an impulsively stretching plate. Accurate series solutions are obtained which are valid for *all* dimensionless time $0 \leqslant \tau < \infty$ in the whole spatial region $0 \leqslant \eta < \infty$. To the best of our knowledge, such kind of series solutions have not been reported. Note that, different from the numerical methods, we can obtain the explicit analytic approximations of $f(\eta,\xi)$, $s(\eta,\xi)$ and $g(\eta,\xi)$, which can help us to understand better the solution structure of the considered problem than the numerical ones.

The present work can be also deemed as a development of the homotopy analysis method. Most previous papers and book on this analytic technique only considered the steady problems governed by differential equation(s). Liao [7], Xu and Liao [9] investigated some unsteady phenomena governed by a partial differential equation. However, in this paper, we applied the homotopy analysis method to study the unsteady boundary-flow problem governed by a set of three partial differential equations, which are much more difficult to do with. In this sense, it is an innovation of the homotopy analysis method.

Acknowledgement

This work is partly sponsored by Program of Shanghai Subject Chief Scientist (Approval No. 05XD14011).

References

[1] B.C. Sakiadis, Boundary-layer behavior on continuous solid surface: I. Boundary-layer equations for two-dimensional and axisymmetric flow, AICHE J. 7 (1961) 26–28.
[2] F.K. Tsou, E.M. Sparrow, R.J. Glodstein, Flow and heat transfer in the boundary layer on a continuous moving surface, Int. J. Heat Mass Transfer 10 (1967) 219–235.
[3] L.E. Erickson, L.T. Fan, V.G. Fox, Heat and mass transfer on a moving continuous flat plate with suction or injection, Ind. Eng. Chem. 5 (1966) 19–25.
[4] T.S. Chen, F.A. Strobel, Buoyancy effects in boundary layer adjacent to a continuous, moving horizontal flat plate, Trans. ASME J. Heat Transfer 102 (1980) 170–172.
[5] A. Chakrabarti, A.S. Gupta, Hydromagnetic flow and heat transfer over a stretching sheet, Quart. Appl. Math. 37 (1979) 73–78.
[6] K. Vajravelu, A. Hadjinicolaou, Convective heat transfer in an electrically conducting fluid at a stretching surface with uniform free stream, Int. J. Engrg. Sci. 35 (1997) 1237–1244.
[7] S.J. Liao, An analytic solution of unsteady boundary-layer flows caused by an impulsively stretching plate, Commun. Nonlinear Sci. Numer. Simulat. 11 (2006) 326–339.
[8] W.T. Cheng, C.N. Huang, Unsteady flow and heat transfer on an accelerating surface with blowing or suction in the absence and presence of a heat source or sink, Chem. Engrg. Sci. 59 (2004) 771–780.
[9] H. Xu, S.J. Liao, Series solutions of unsteady magnetohydrodynamic flows of non-Newtonian fluids caused by an impulsively stretching plate, J. Non-Newton. Fluid Mech. 159 (2005) 46–55.
[10] P.J. Hilton, An Introduction to Homotopy Theory, Cambridge University Press, 1953.
[11] S. Sen, Topology and Geometry for Physicists, Academic Press, Florida, 1983.
[12] E.I. Grigolyuk, V.I. Shalashilin, Problems of Nonlinear Deformation: The Continuation Method Applied to Nonlinear Problems in Solid Mechanics, Kluwer Academic Publishers, Dordrecht, 1991.
[13] J.C. Alexander, J.A. Yorke, The homotopy continuation method: numerically implementable topological procedures, Trans. Amer. Math. Soc. 242 (1978) 271–284.
[14] S.J. Liao, The proposed homotopy analysis techniques for the solution of nonlinear problems, PhD dissertation, Shanghai Jiao Tong University, Shanghai, 1992 (in English).
[15] S.J. Liao, A second-order approximate analytical solution of a simple pendulum by the Process Analysis method, Trans. ASME J. Appl. Mech. 59 (1992) 970–975.
[16] S.J. Liao, A kind of approximate solution technique which does not depend upon small parameters: a special example, Int. J. Non-Linear Mech. 30 (1995) 371–380.
[17] S.J. Liao, A kind of approximate solution technique which does not depend upon small parameters (II): an application in fluid mechanics, Int. J. Non-Linear Mech. 32 (1997) 815–822.
[18] S.J. Liao, An explicit, totally analytic approximation of Blasius viscous flow problems, Int. J. Non-Linear Mech. 34 (1999) 759–778.
[19] S.J. Liao, On the homotopy analysis method for nonlinear problems, Appl. Math. Comput. 147 (2004) 499–513.
[20] A.M. Lyapunov (1892), General Problem on Stability of Motion, Taylor & Francis, London, 1992 (English translation).
[21] G. Adomian, Nonlinear stochastic differential equations, J. Math. Anal. Appl. 55 (1976) 441–452.
[22] A.V. Karmishin, A.T. Zhukov, V.G. Kolosov, Methods of Dynamics Calculation and Testing for Thin-Walled Structures, Mashinostroyenie, Moscow, 1990 (in Russian).
[23] S.J. Liao, Beyond Perturbation: Introduction to the Homotopy Analysis Method, Chapman & Hall/CRC Press, Boca Raton, 2003.
[24] J.H. He, Homotopy perturbation technique, Comput. Methods Appl. Mech. Engrg. 178 (1999) 257–262.
[25] S.J. Liao, Comparison between the homotopy analysis method and homotopy perturbation method, Appl. Math. Comput. 169 (2005) 1186–1194.
[26] S.J. Liao, A uniformly valid analytic solution of 2D viscous flow past a semiinfinite flat plate, J. Fluid Mech. 385 (1999) 101–128.
[27] S.J. Liao, A. Campo, Analytic solutions of the temperature distribution in Blasius viscous flow problems, J. Fluid Mech. 453 (2002) 411–425.
[28] S.J. Liao, An analytic approximation of the drag coefficient for the viscous flow past a sphere, Int. J. Non-Linear Mech. 37 (2002) 1–18.

[29] S.J. Liao, On the analytic solution of magnetohydrodynamic flows of non-Newtonian fluids over a stretching sheet, J. Fluid Mech. 488 (2003) 189–212.
[30] J. Cheng, S.J. Liao, I. Pop, Analytic series solution for unsteady mixed convection boundary layer flow near the stagnation point on a vertical surface in a porous medium, Transport in Porous Media 61 (2005) 365–379.
[31] S.J. Liao, A new branch of solutions of boundary-layer flows over a permeable stretching plate, Int. J. Heat Mass Transfer 48 (2005) 2529–2539.
[32] S.J. Liao, E. Magyari, Exponentially decaying boundary layers as limiting cases of families of algebraically decaying ones, ZAMP, in press.
[33] H.S. Takhar, A.J. Chamkha, G. Nath, Unsteady three-dimensional MHD-boundary-layer flow due to the impulsive motion of a stretching surface, Acta Mech. 146 (2001) 59–71.
[34] J.C. Williams, T.H. Rhyne, Boundary layer development on a wedge impulsively set into motion, SIAM J. Appl. Math. 38 (1980) 215–224.